Catalysis Today 161 (2011) 35–40

Contents lists available at ScienceDirect

Catalysis Today

journal homepage: www.elsevier.com/locate/cattod

Preparation of Sm-loaded brookite TiO_2 photocatalysts

A. Di Paola [a,*], M. Bellardita [a], G. Marcì [a], L. Palmisano [a], F. Parrino [a], R. Amadelli [b]

[a] "Schiavello-Grillone" Photocatalysis Group, Dipartimento di Ingegneria Elettrica, Elettronica e delle Telecomunicazioni, Università di Palermo, Viale delle Scienze, 90128 Palermo, Italy
[b] Dipartimento di Chimica and ISOFCNR, Università degli Studi di Ferrara, Via Luigi Borsari 46, 44100 Ferrara, Italy

ARTICLE INFO

Article history:
Received 25 May 2010
Received in revised form 19 October 2010
Accepted 7 November 2010
Available online 14 December 2010

Keywords:
Photocatalysis
TiO_2
Brookite
Loaded brookite

ABSTRACT

Pure and Sm-loaded brookite nanoparticles and thin films were prepared using $TiCl_4$ as precursor of TiO_2. The samples were characterized by X-ray diffraction (XRD), specific surface area (SSA) determination, diffuse reflectance spectroscopy (DRS) and photoluminescence (PL) measurements. The photocatalytic activity of the powders was investigated by employing the photodegradation of 4-nitrophenol in a liquid–solid system whilst the photoreactivity of the films was tested by evaluating the rate of degradation of 2-propanol in a gas–solid system. Loading with Sm resulted in a significant improvement of the photoreactivity of brookite and the beneficial effect was attributed to an increased separation efficiency of the photogenerated electron–hole pairs. The content of samarium was an important factor affecting the photocatalytic activity. The optimum amount of samarium was 1% for the powders and 0.1% for the films. There is a relationship between PL spectra and photoactivity, namely, the lower the PL intensity, the higher the photocatalytic activity.

1. Introduction

Titanium dioxide is the most widely studied photocatalyst for the oxidative degradation of organic pollutants present in wastewater effluents or in air [1–3]. TiO_2 has many attractive characteristics such as chemical stability, non toxicity and low cost [4] but its photocatalytic efficiency is limited by a high rate of recombination of the photogenerated electron–hole pairs.

The main crystalline modifications of TiO_2 are rutile (tetragonal), anatase (tetragonal) and brookite (orthorhombic). All three crystalline structures consist of deformed TiO_6 octahedra connected differently by corners and edges [5]. Anatase and rutile are the forms more frequently studied because pure brookite is rather difficult to be prepared.

Pure brookite was prevalently prepared from titanium(IV) compounds via hydrothermal treatments at high temperatures [6–11]. Brookite nanoparticles were synthesized in mild conditions of temperature and pressure [12–14] or by employing titanium(III) compounds as TiO_2 precursors [15–17]. Only a few papers have concerned with the preparation of brookite films [18–21].

The photoactivity of TiO_2 can be improved by surface functionalization [22–24] or by doping with metallic and non-metallic species. Many controversial results are reported in the literature because the photoactivity of the resulting catalysts depends both on the dopant and the substrate to be photodegraded. Choi et al. [25] studied the effect of 21 different metal ion dopants both for the oxidation of $CHCl_3$ and for the reduction of CCl_4. The results showed that some metal ions increased the photoactivity of TiO_2 whilst others were detrimental. The photooxidation of various aliphatic and aromatic organic compounds revealed that the methanoic acid degradation was enhanced by the presence of cobalt ions whilst the sample doped with W was the most efficient for the mineralization of benzoic acid and 4-nitrophenol [26]. An explanation was proposed by taking into account the nature of the reacting molecules and the acid–base and electronic properties of the photocatalysts.

Recently, lanthanide-doped TiO_2 samples have received an increasing attention for their enhanced photocatalytic properties [27–43]. The increase in activity was attributed to a higher adsorption and reduction of the electron–hole recombination. Ranjit et al. [27] prepared a series of lanthanide ions doped TiO_2 (Ln^{3+} = Eu^{3+}, Pr^{3+}, Yb^{3+}) which revealed a substantially enhanced activity for the photodegradation of p-nitrobenzoic acid, p-chlorophenoxyacetic acid, aniline, salycilic acid and trans-cinnamic acid. Various lanthanide ions with different 4f electronic configurations were studied as dopants of TiO_2 for the degradation of phenol [28], 2-mercaptobenzothiazole [29], nitrite [30] and various dyes [31–41]. All lanthanide-doped samples exhibited an improvement of photoactivity with respect to undoped TiO_2. The introduction of lanthanide ions extended the optical absorption of the doped samples to longer wavelengths enhancing the photocatalytic activity under UV or visible light illumination [36–42].

Sm-doped TiO_2 is an attractive material for its spectroscopic properties [43–45] and good photocatalytic performances [30–39]. The photoactivity of the TiO_2 samples doped with samarium ions

* Corresponding author. Tel.: +39 091 238 63729.
E-mail address: agatino.dipaola@unipa.it (A. Di Paola).

0920-5861/$ – see front matter © 2010 Elsevier B.V. All rights reserved.
doi:10.1016/j.cattod.2010.11.016

has been generally compared to that of other lanthanide-doped TiO_2 materials [30–36] and some researchers [30,34–39] have studied the effect of the samarium content on the photocatalytic activity of TiO_2. Anatase is the crystallized phase usually doped with lanthanide ions and only few works have concerned a mixture of anatase and rutile doped with samarium [37,38]. To the best of our knowledge no studies on the photocatalytic activity of brookite samples containing samarium have ever been published either in liquid–solid or in gas–solid systems.

In this study we report on the synthesis of Sm-loaded brookite powders and films obtained by a sol–gel method. The preparation method is very simple and does not require the use of expensive thermal or hydrothermal treatments. The photodegradation of 4-nitrophenol (4-NP) was used to evaluate the reactivity of the powders whilst the films were tested for the photodegradation of 2-propanol. The effect of the content of samarium on the photocatalytic efficiency was also studied.

2. Experimental

2.1. Preparation of the samples

2.1.1. Powders

15 mL of $TiCl_4$ (Fluka 98%) was added dropwise to a solution containing 630 mL of demineralized water and 240 mL of concentrated hydrochloric acid. The hydrolysis reaction was highly exothermic and released fumes of HCl. The solution obtained after continuous stirring was heated in a closed bottle and aged at 100 °C in an oven for 48 h. The resultant precipitate contained a mixture of brookite and rutile. Pure brookite nanoparticles were separated by peptization by removing many times the surnatant and adding water to restore the initial solution volume. After a few washings, a dispersion of brookite particles formed whilst the rutile phase remained as precipitate [46]. The dispersion was recovered and the washing treatment was repeated till the liquid on the solid rutile became transparent. All dispersions containing the brookite particles were collected and dried under vacuum at 55 °C.

Samarium loading was accomplished by adding Sm_2O_3 (Aldrich 99.9%) to the solution obtained by dissolution of $TiCl_4$. The following code was used for the loaded samples: B(*x*%Sm), where *x*% indicates the nominal percentage of metal with respect to total amount of TiO_2.

2.1.2. Films

Bare TiO_2 films were prepared by immersing microscopy glasses (75 mm × 25 mm × 1 mm) in the brookite dispersion obtained by peptization of the mixture of brookite and rutile. The withdrawal speed was 60 mm/min. After each coating the films were first dried at room temperature for 15 min and then calcined at 400 °C for 2 h. The treatment was repeated 10 times. The samarium loaded films were prepared as above described for bare TiO_2 but in the presence of Sm_2O_3.

2.2. Characterizations of the samples

XRD patterns of the powders were recorded at room temperature by a Philips powder diffractometer using the CuKα radiation and 2θ scan rate of 2°/min. The diffractograms of the films were obtained by a D8 Bruker X-ray diffractometer with a 2θ scan rate of 0.01°/s and an incident angle of 0.5°. The specific surface areas of the powders were determined in a Flow Sorb 2300 apparatus (Micromeritics) using the single-point BET method. Visible-ultraviolet spectra were obtained by diffuse reflectance spectroscopy by using a Shimadzu UV-2401 PC instrument. $BaSO_4$ was the reference sample and the spectra were recorded in the range 200–800 nm. Photoluminescence spectra were recorded at room temperature with a Jobin Yvon Spex Fluoromax II spectrofluorimeter equipped with a Hamamatsu R3896 photomultiplier.

To determine the adsorption behavior of the Sm-loaded samples, 0.06 g of powder was added to 100 mL of a 20 mg L^{-1} aqueous solution of 4-nitrophenol. The suspension was stirred for 3 h in the dark to ensure the equilibration of the substrate over the catalyst surface and the amount of adsorbed 4-nitrophenol was calculated by comparing the concentration before and after stirring. The catalyst was separated from the solution by filtration through a 0.1 μm Teflon membrane (Whatman). Some drops of a 1 M NaOH solution were added before filtration to obtain agglomeration of the particles. The quantitative determination of 4-NP was performed by measuring its absorption at 315 nm with a spectrophotometer Shimadzu UV-2401 PC.

2.3. Photoreactivity experiments

A Pyrex batch photoreactor of cylindrical shape containing 0.5 L of aqueous suspension was used. A 125 W medium pressure Hg lamp (Helios Italquartz, Italy) was immersed within the photoreactor and the photon flux emitted by the lamp was $\Phi_i = 13.5$ mW cm^{-2}. O_2 was continuously bubbled for ca. 0.5 h before switching on the lamp and throughout the occurrence of the photoreactivity experiments. The temperature inside the reactor was ca. 30 °C. The amount of catalyst was 0.6 g L^{-1} and the initial 4-nitrophenol (BDH) concentration was 20 mg L^{-1}. Samples of 5 mL were withdrawn at fixed intervals of time with a syringe, and the catalyst was separated from the solution by filtration through 0.1 μm Teflon membranes (Whatman).

The photoreactivity of the films was evaluated in a cylindrical Pyrex batch photoreactor ($V = 0.9$ dm^3) where two juxtaposed coated glasses were placed. The films were irradiated from the top by a 500 W medium pressure Hg lamp. The irradiance at the film surface was 1.3 mW cm^{-2}. A water filter was interposed between the lamp and the photoreactor to cut the infrared radiation. O_2 was fluxed in the reactor for ca. 0.5 h before turning off the inlet and outlet valves. Subsequently, 2-propanol was injected into the reactor and the lamp was switched on. 0.5 mL of the mixture was withdrawn at different irradiation times using a gas-tight syringe. 2-Propanol and propanone concentrations were measured by a GC-17A Shimadzu gas chromatograph equipped with a HP-1 column and a flame ionization detector. CO_2 was detected by a HP 6890 Series GC System equipped with a packed column GC 60/80 Carboxen-1000.

3. Results and discussion

3.1. Characterization of the samples

X-ray measurements confirmed that the solids separated after selective peptization of the precipitate obtained by thermolysis of the $TiCl_4$ solution at 100 °C for 48 h contained only single-phase rutile or brookite [46]. The identity of the brookite polymorph was also verified by Raman spectroscopy. All peaks of the Raman spectrum of the as-prepared brookite powder were consistent with those of natural brookite crystals [47].

No peaks related to other TiO_2 phases such as anatase or rutile were observed in the diffractograms of the brookite samples loaded with various samarium contents. The peaks were rather broad, characteristic of partially crystalline powders with nanosized structure. The lack of appreciable diffraction peaks due to samarium oxide indicates a high degree of dispersion of the loaded metal onto the support, probably because the preparation temperature of the samples was too low to enable the formation of a "bulk" oxide. The Raman spectra of the loaded samples were similar to

Table 1
Crystallite size (ϕ), specific surface area (SSA), percentage of adsorbed 4-NP (%), band gap (E_g) and initial reaction rate (r_0) of the various samples.

Sample	ϕ (nm)	SSA ($m^2\,g^{-1}$)	%	E_g (eV)	$r_0 \times 10^9$ ($mol\,L^{-1}\,s^{-1}$)
Brookite	14.8	70	0.6	3.27	15.0
B(0.1%Sm)	13.9	80	1.3	3.29	18.4
B(0.5%Sm)	13.0	73	2.8	3.28	20.7
B(1%Sm)	12.3	74	2.6	3.28	26.3
B(2%Sm)	11.7	83	2.9	3.29	12.4

that of brookite but slightly shifted, as already found for anatase nanoparticles doped with Tb, Eu or Sm [34]. The shift of the peaks should result from crystal structure modifications, such as oxygen vacancies [48].

Table 1 reports the diameter of the crystallites of the various samples, estimated by means of the Scherrer equation from the broadening of the (1 2 1) XRD peak of brookite. All the samples were nanocrystalline and the mean diameter of the crystallites was lower than 15 nm. The particle size of the Sm-loaded brookite crystallites was lower than that of unloaded brookite and decreased with increasing the nominal content of samarium. The decrease may be attributed to the presence of Sm–O–Ti bonds in the doped samples, which inhibits the growth of crystal grains [30]. Similar inhibitory effect was found in nanosized TiO_2 doped with various lanthanide ions [30,34–39].

The specific surface areas of the various samples are reported in Table 1. The SSA values ranged between 70 and 83 $m^2\,g^{-1}$ and the surface areas of the Sm-loaded samples were higher than that of undoped brookite.

Fig. 1 shows the XRD patterns of pure brookite and B(1%Sm) calcined at different temperatures. The brookite structure was conserved till 750 °C for both samples. At 800 °C a strong peak corresponding to rutile appeared in the diffractogram of the unloaded sample whilst the peaks of brookite were almost completely absent. Differently, only a little peak of rutile appeared and the peak intensities of brookite slightly decreased when B(1%Sm) was calcined at 800 °C. At 850 °C the transformation of brookite to rutile was practically complete for both samples even if very small peaks of brookite could be appreciated in the diffractogram of the sample containing samarium. At 900 °C the XRD patterns revealed only peaks of rutile. These results indicate that the presence of samarium inhibits the phase transformation from brookite to rutile and increases the temperature of phase transition. An inhibition of the transformation from anatase to rutile was previously reported for phosphate-modified nanocrystalline titania films [22], for various lanthanide [28,48] and Sm [37–39] doped TiO_2 samples. The inhibitory effect was ascribed to the stabilization of the anatase phase through the formation of Ti–O–P [22] or Ti–O–rare earth element bonds [48]. The formation of Ti–O–Sm bonds can be also invoked for the Sm-loaded brookite samples.

Fig. 2 shows the diffuse reflectance spectra of pure and Sm-loaded brookite samples. The spectra were quite similar to each other but the curves of the samples containing samarium were slightly blue shifted. Similar results were obtained with Sm-loaded anatase samples obtained by boiling an aqueous solution of $TiCl_4$ [42]. It is worth noting that the results reported in the literature are quite controversial. The spectra of some rare earth metal-doped TiO_2 showed red shifts in the band gap transition [30,34–39] that were attributed to the charge transfer transition between the rare earth ion f electrons and the TiO_2 conduction or valence band. In particular, Xu et al. [30] found that the spectrum of the samarium doped sample exhibited the smallest red shift with respect to the spectra of various lanthanide doped TiO_2 nanoparticles. Differently, Jing et al. [28] found a blue shift of the spectrum of La doped TiO_2 nanoparticles that was attributed to the quantum size effect [49].

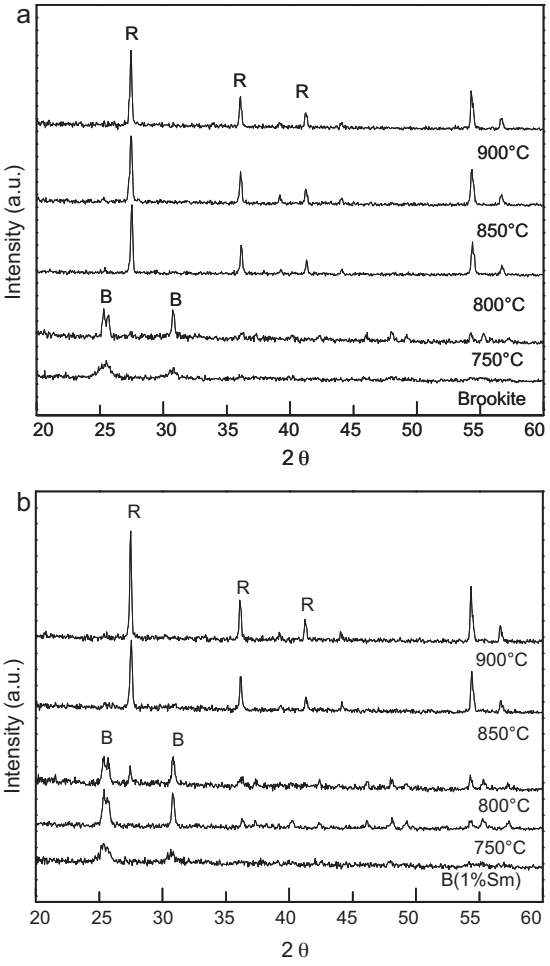

Fig. 1. XRD patterns of (a) pure brookite and (b) B(1%Sm), calcined at different temperatures.

The band gap energies of the various samples were estimated from the tangent lines in the plots of the modified Kubelka–Munk function, $[F(R'_\infty)h\nu]^{1/2}$, versus the energy of the exciting light [50]. The presence of samarium little influenced the band gap of the sam-

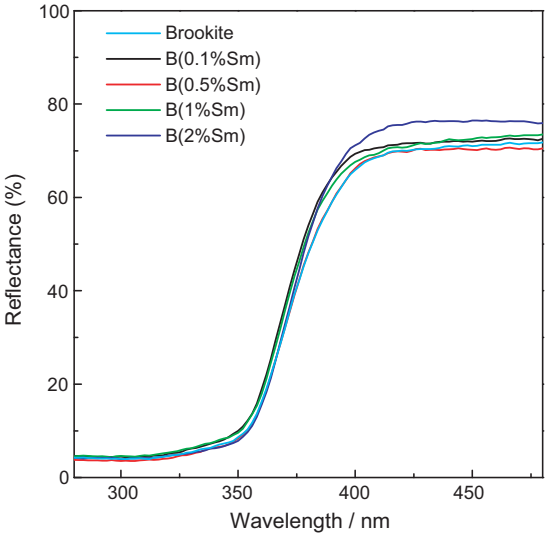

Fig. 2. Diffuse reflectance spectra of brookite loaded with various amounts of samarium.

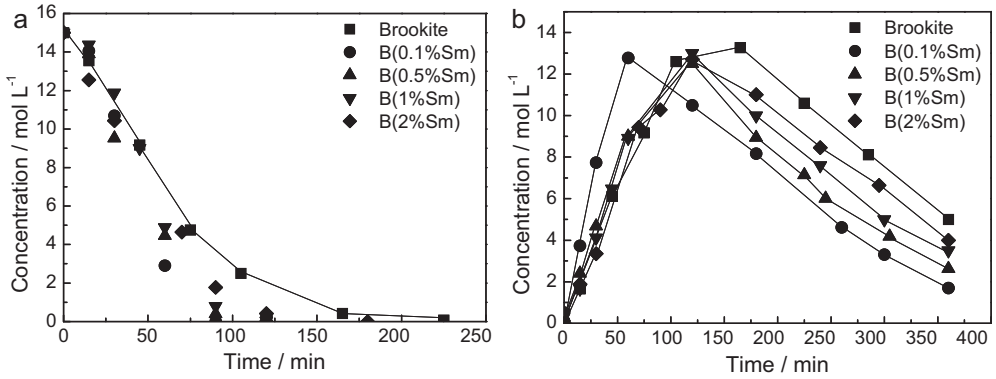

Fig. 3. Photocatalytic degradation of 2-propanol (a) and variation of the propanone concentration (b) in the presence of Sm-loaded brookite films.

ples whose values ranged between 3.28 and 3.29 eV (see Table 1) and were very near to that of brookite (3.27 eV).

The adsorption of substrate on the surface of a sample is an important parameter to evaluate its catalytic activity. The saturation amount of 4-nitrophenol adsorbed on the samples containing different contents of samarium is reported in Table 1. The percentage of 4-nitrophenol was evaluated from $(1 - C/C_0) \times 100$ where C and C_0 represent the equilibrium concentration and the initial concentration of 4-nitrophenol, respectively. All the Sm-loaded brookite samples showed an adsorption capacity slightly higher than that of pure brookite. The improvement is probably ascribable to the formation of Lewis acid–base complexes between the samarium ions and the functional groups of 4-NP [27].

3.2. Photoreactivity experiments

3.2.1. Powders

The disappearance of 4-nitrophenol was followed by determining the concentration of the substrate at various time intervals. The degradation rate, r_0, was calculated from the initial slope of the concentration versus time profiles. The various values of r_0 are reported in Table 1. The results revealed that the loaded samples were always more active than pure brookite. In particular, the photoactivity increased with increasing the nominal concentration of samarium, reached a maximum value and afterwards decreased. The best results were obtained with B(1%Sm). Optimal values of samarium content were previously found for Sm^{3+}-doped anatase [30,39] or (anatase + rutile) [37] samples. The differences in the optimum concentration are probably related to the different routes of preparation of the samples.

The highest photoreactivity cannot be ascribed to the largest specific surface areas and/or the highest adsorption capacity of the Sm-loaded samples. Indeed, the differences of SSA are rather small and the loaded samples with the lowest specific areas were the most active. Moreover, the highest adsorption capacity of B(0.5%Sm) and B(2%Sm) did not lead to a higher photoactivity.

The enhancement of photoreactivity of TiO_2 samples doped with samarium has been attributed to an increased separation of the photogenerated electron–hole pairs [30,37,42]. The Sm^{3+} ions present on the particles can interact with the brookite surface trapping electrons that can be transferred to the adsorbed O_2 molecules to produce the very oxidant superoxide radical ion O_2^-, according to the following reactions:

$$Sm^{3+} + e^- \rightarrow Sm^{2+} \quad \text{(electron trapping)}$$

$$Sm^{2+} + O_2 \rightarrow Sm^{3+} + O_2^- \quad \text{(electron transfer)}$$

Sm^{2+} ions, with 6f electrons, are very instable so that the electrons can be easily detrapped and transferred to the oxygen molecules reducing the electron–hole recombination and thus enhancing the photocatalytic activity. Moreover, the presence of samarium ions is beneficial because of the ability of the f orbitals to form Lewis acid–base complexes with the substrate [27]. In such manner the substrate is sequestered on the surface of TiO_2 rendering faster its photodegradation.

According to Pleskov [51] the value of the space charge region potential for an efficient separation of the photoinduced electron–hole pairs must be higher than 0.2 V. As the concentration of loading ion increases, the surface barrier becomes higher and the space charge region becomes narrower so that the efficiency of electron–hole separation increases and the photoactivity is enhanced [30]. Anyway, beyond a certain doping level the space charge layer becomes very narrow and the penetration depth of light exceeds the space charge layer favouring the recombination of the electron–hole pairs and the photoactivity is reduced. Thus, there is an optimum degree of loading at which photoactivity is maximum.

3.2.2. Films

A serious drawback of the employment of photocatalyst suspensions is the necessity to separate the solid by filtration after the reaction. A suitable alternative is the immobilization of the photocatalyst on solid supports. Experiments were carried out by depositing thin films of brookite or Sm-loaded brookite on glass slides. The photocatalytic activity of the various samples was evaluated using the photodegradation of 2-propanol. The main intermediate product was propanone that was furtherly oxidized to CO_2 [52,53].

Fig. 3a shows the decrease of 2-propanol concentration under UV irradiation in the presence of brookite films containing different percentages of samarium. The photoactivity of all loaded samples was larger than that of the bare brookite film and the most active sample was B(0.1%Sm). As shown in Fig. 3b, the disappearance of 2-propanol was accompanied by a continuous increase of propanone whose amount reached a maximum and then slowly decreased to zero. Propanone was always completely mineralized and the CO_2 concentration reached its stoichiometric value.

The different optimum contents of samarium found for powders and films probably depend on the different adsorption capacities of the two types of catalysts. A chemical adsorption between samarium ions and functional groups of 4-nitrophenol can be invoked in the liquid–solid system, whilst a physical adsorption of 2-propanol is predictable in the gas–solid regimen.

3.3. Photoluminescence measurements

Photoluminescence represents an interesting searching approach to tracking the reactivity of light generated charges with

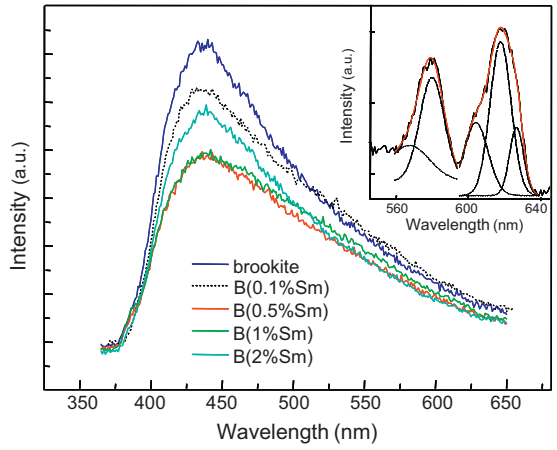

Fig. 4. Room temperature photoluminescence spectra of pure and Sm-loaded brookite samples (λ_{exc} = 340 nm). The inset shows emission spectra due to Sm^{3+} in loaded anatase nanoparticles (see text for explanation).

species present in the fluid phase [54]. From a general point of view, PL originates from radiative recombination of photogenerated electrons and holes and is extremely sensitive to surface phenomena. Specifically, light emission from charge recombination can be associated with (i) self-trapped excitons; (ii) oxygen vacancies; (iii) surface states [55]. According to several literature studies, PL can also supply information about the relationships between surface characteristics and photocatalytic activity. However, for the particular case of TiO_2, the relationship between PL intensity and photocatalytic activity is not univocal and largely depends on the nature of the photoluminescence phenomenon [55]. There are situations in which a particular treatment of the starting material brings about an increase of the photocatalytic efficiency and a corresponding decrease of PL due to band gap recombination [56] whilst in other cases such enhanced efficiency is accompanied by an increase of PL originated by the presence of a large number of vacancies and defects able to bind excitons [28].

Room temperature emission PL spectra of pure and Sm-loaded brookite powders upon ultra band gap excitation (λ = 340 nm) are shown in Fig. 4. The shape of the spectra was similar indicating that the presence of samarium does not give rise to new PL phenomena. Emission in the range 400–500 nm was also typically observed for undoped anatase samples, and these signals were assigned to the recombination of surface trapped electrons with holes in the valence band [57–60]. Loading brookite with Sm leads to a decrease of PL intensity for doping degrees between 0.1 and 1%. Conversely, for higher amounts of samarium (2%) the PL intensity increases again but remains lower than that measured for pristine brookite, which can be probably explained by a surface segregation of metal species leaving wide portions of the surface unmodified. Such segregation phenomena have been reported for the case of TiO_2 doped by 2% cobalt [61]. An explanation based on an increase of the number of vacancies is unlikely since a significant replacement of Ti by Sm appears difficult both due to the larger radius of the latter [30] and to the low preparation temperature of the samples. The trend described for the PL intensity closely reflects the observed photocatalytic efficiency as a function of the loading degree by samarium.

Notably at variance with the behavior shown in Fig. 4, Xiao et al. [38] found that doping of nanocrystalline anatase with Sm up to 0.5% increased the PL intensity, which was ascribed to an increase in the amount of surface oxygen vacancies. A rise of PL intensity as a function of doping up to 0.5% was paralleled by an enhancement of the photocatalytic activity for methylene blue degradation. The results of this investigation do not indicate that loading introduces extra oxygen vacancies.

It is noteworthy that no new PL signals were observed in the wavelength range from 400 to 650 nm whilst several investigations [44,45,62] on samarium-doped TiO_2 report the presence of new peaks between 550 and 650 nm which were assigned to energy transfer from excited host TiO_2 to samarium. Indeed, as shown by the inset of Fig. 4, these peaks were found in the PL spectra of Sm-loaded anatase samples that were prepared by a sol–gel method and calcined at 700 °C according to Ref. [45]. Thus, the preparation method and thermal post-treatment have an evident influence on the properties of the resulting photocatalysts.

4. Conclusions

Bare and Sm-loaded brookite powders and films were prepared under mild experimental conditions. The photoactivity of the loaded samples was generally higher than that of pristine brookite. The photoactivity increased with increasing the concentration of samarium, reached a maximum value and afterwards decreased. The presence of samarium inhibited the transformation from brookite to rutile and reduced the intensity of the PL spectra. There is a relationship between PL spectra and photoactivity, namely, the lower the PL intensity, the higher the photocatalytic activity.

References

[1] D.F. Ollis, H. Al-Ekabi (Eds.), Photocatalytic Purification and Treatment of Water and Air, Elsevier, Amsterdam, 1993.
[2] M.R. Hoffmann, S.T. Martin, W. Choi, D.W. Bahnemann, Chem. Rev. 95 (1995) 69.
[3] A. Fujishima, T. Rao, D.A. Tryk, J. Photochem. Photobiol. C: Photochem. Rev. 1 (2000) 1.
[4] A. Fujishima, K. Hashimoto, T. Watanabe, TiO_2 Photocatalysis: Fundamentals and Applications, Bkc, Tokyo, 1999.
[5] X. Bokhimi, A. Morales, M. Aguilar, J.A. Toledo-Antonio, F. Pedraza, Int. J. Hydrogen Energy 26 (2001) 1279.
[6] T. Nagase, T. Ebina, T. Iwasaki, H. Hayashi, Y. Onodera, M. Chatterjee, Chem. Lett. (1999) 911.
[7] H. Kominami, M. Kohno, Y. Kera, J. Mater. Chem. 10 (2000) 1151.
[8] H. Kominami, J.-I. Kato, S.-Y. Murakami, Y. Ishii, M. Kohno, K.-I. Yabutani, T. Yamamoto, Y. Kera, M. Inoe, T. Inui, B. Ohtani, Catal. Today 84 (2003) 181.
[9] Y. Zheng, E. Shi, S. Cui, W. Li, X. Hu, J. Mater. Sci. Lett. 19 (2000) 1445.
[10] W. Luo, S.F. Yang, Z.C. Wang, R. Ahuja, B. Johansson, J. Liu, G.T. Zou, Solid State Commun. 133 (2005) 49.
[11] K. Tomita, V. Petrykin, M. Kobayashi, M. Shiro, M. Yoshimura, M. Kakihana, Angew. Chem. Int. Ed. 45 (2006) 2378.
[12] A. Pottier, C. Chanéac, E. Tronc, L. Mazerolles, J.P. Jolivet, J. Mater. Chem. 11 (2001) 1112.
[13] J.H. Lee, Y.S. Yang, J. Mater. Sci. 41 (2006) 557.
[14] B.I. Lee, X. Wang, R. Bhave, M. Hu, Mater. Lett. 60 (2006) 1179.
[15] B. Ohtani, J.-I. Handa, S.-I. Nishimoto, T. Kagiya, Chem. Phys. Lett. 120 (1985) 292.
[16] J.-G. Li, C. Tang, D. Li, H. Haneda, T. Ishigaki, J. Am. Ceram. Soc. 87 (2004) 1358.
[17] S. Bakardjieva, V. Stengl, L. Szatmary, J. Subrt, J. Lukac, N. Murafa, D. Niznansky, K. Cizek, J. Jrkovsky, N. Petrova, J. Mater. Chem. 16 (2006) 1709.
[18] M. Koelsch, S. Cassaignon, J.F. Guillemoles, J.-P. Jolivet, Thin Solid Films 403–404 (2002) 312.
[19] M. Koelsch, S. Cassaignon, C. Ta Thanh Minh, J.F. Guillemoles, J.-P. Jolivet, Thin Solid Films 451–452 (2004) 86.
[20] A. Di Paola, M. Addamo, M. Bellardita, E. Cazzanelli, L. Palmisano, Thin Solid Films 515 (2007) 3527.
[21] M. Addamo, M. Bellardita, A. Di Paola, L. Palmisano, Chem. Commun. (2006) 4943.
[22] L. Kőrösi, A. Oszkó, G. Galbács, A. Richardt, V. Zöllmer, I. Dékány, Appl. Catal. B 77 (2007) 175.
[23] L. Kőrösi, S. Papp, J. Ménesi, E. Illés, V. Zöllmer, A. Richardt, I. Dékány, Colloids Surf. A: Physicochem. Eng. Aspects 319 (2008) 136.
[24] P. Calza, E. Pelizzetti, K. Mogyorósi, R. Kun, I. Dékány, Appl. Catal. B 72 (2007) 314.
[25] W. Choi, A. Termin, M.R. Hoffmann, J. Phys. Chem. 98 (1994) 13669.
[26] A. Di Paola, E. García-López, S. Ikeda, G. Marcì, B. Ohtani, L. Palmisano, Catal. Today 75 (2002) 87.
[27] K.T. Ranjit, H. Cohen, I. Willer, S. Bossmann, A.M. Braun, J. Mater. Sci. 34 (1999) 5273.

[28] L. Jing, X. Sun, B. Xin, B. Wang, W. Cai, H. Fu, J. Solid State Chem. 177 (2004) 3375.
[29] F.B. Li, X.Z. Li, M.F. Hou, K.W. Cheah, W.C.H. Choy, Appl. Catal. A 285 (2005) 181.
[30] A.-W. Xu, Y. Gao, H.-Q. Liu, J. Catal. 207 (2002) 151.
[31] Y. Wang, H. Cheng, L. Zhang, Y. Hao, J. Ma, B. Xu, W. Li, J. Mol. Catal. A: Chem. 151 (2000) 205.
[32] M. Bettinelli, A. Speghini, D. Falcomer, M. Daldosso, V. Dallacasa, L. Romanò, J. Phys. Condens. Matter 18 (2006) S2149.
[33] C.-H. Liang, F.-B. Li, C.-S. Liu, J.-L. Lü, X.-G. Wang, Dyes Pigm. 76 (2008) 477.
[34] M. Saif, M.S.A. Abdel-Mottaleb, Inorg. Chim. Acta 360 (2007) 2863.
[35] Z.M. El-Bahy, A.A. Ismail, R.M. Mohamed, J. Hazard. Mater. 166 (2009) 138.
[36] V. Štengl, S. Bakardjieva, N. Murafa, Mater. Chem. Phys. 114 (2009) 217.
[37] Q. Xiao, Z. Si, Z. Yu, G. Qiu, J. Alloys Compd. 450 (2008) 426.
[38] Q. Xiao, Z. Si, J. Zhang, C. Xiao, Z. Yu, G. Qiu, J. Mater. Sci. 42 (2007) 9194.
[39] J. Shi, J. Zheng, Y. Hu, Y. Zhao, Environ. Eng. Sci. 25 (2008) 489.
[40] Y. Xie, C. Yuan, X. Li, Colloids Surf. A: Physicochem. Eng. Aspects 252 (2005) 87.
[41] Y. Xie, C. Yuan, X. Li, Mater. Sci. Eng. B 117 (2005) 325.
[42] M. Bellardita, M. Addamo, A. Di Paola, L. Palmisano, Chem. Phys. 339 (2007) 94.
[43] V. Kiisk, I. Sildos, S. Lange, V. Reedo, T. Tätte, M. Kirm, J. Aarik, Appl. Surf. Sci. 247 (2005) 412.
[44] V. Kiisk, V. Reedo, M. Karbowiak, M.G. Brik, I. Sildos, J. Phys. D: Appl. Phys. 42 (2009) 125107.
[45] L. Hu, H. Song, G. Pan, B. Yan, R. Qin, Q. Dai, L. Fan, S. Li, X. Bai, J. Lumin. 127 (2007) 371.
[46] A. Di Paola, G. Cufalo, M. Addamo, M. Bellardita, R. Campostrini, M. Ischia, R. Ceccato, L. Palmisano, Colloids Surf. A: Physicochem. Eng. Aspects 317 (2008) 366.
[47] G.A. Tompsett, G.A. Bowmaker, R.P. Cooney, J.B. Metson, K.A. Rodgers, J.M. Seakins, J. Raman Spectrosc. 26 (1995) 57.
[48] J. Lin, J.C. Yu, J. Photochem. Photobiol. A 116 (1998) 63.
[49] L.E. Brus, J. Phys. Chem. 90 (1986) 2555.
[50] Y.I. Kim, S.J.E. Atherton, S. Brigham, T.E. Mallouk, J. Phys. Chem. 97 (1993) 11802.
[51] Y.V. Pleskov, Sov. Electrochem. 17 (1981) 1.
[52] Y. Ohko, A. Fujishima, K. Hashimoto, J. Phys. Chem. B 102 (1998) 1724.
[53] S. Hager, R. Bauer, Chemosphere 38 (1999) 1549.
[54] N. Serpone, D. Lawless, R. Khairutdinov, J. Phys. Chem. 99 (1995) 16646.
[55] L. Jing, Y. Qu, B. Wang, S. Li, B. Jiang, L. Yang, W. Fu, H. Fu, J. Sun, Sol. Energy Mater. Sol. Cells 90 (2006) 1773.
[56] F.B. Li, X.Z. Li, Appl. Catal. A 228 (2002) 15.
[57] Y. Wang, S. Zhang, X. Wu, Nanotechnology 15 (2004) 1162.
[58] L. Jing, X. Sun, W. Cai, Z. Xu, Y. Du, H. Fu, J. Phys. Chem. Solids 64 (2003) 615.
[59] D. Noguchi, Y. Kawamata, T. Nagatomo, J. Electrochem. Soc. 152 (2005) D124.
[60] F. Dong, W. Zhao, Z. Wu, S. Guo, J. Hazard. Mater. 162 (2009) 763.
[61] R. Amadelli, L. Samiolo, A. Maldotti, A. Molinari, M. Valigi, D. Gazzoli, Int. J. Photoenergy (2008) (Article ID 853753, 9 pages).
[62] K.L. Frindell, M.H. Bartl, M.R. Robinson, G.C. Bazan, A. Popitsch, G.D. Stucky, J. Solid State Chem. 172 (2003) 81.